AUTHOR'S POST PRINT (Romeo Colour: Green)
MSSU: Microgravity & Space Station Utilization (ISSN: 0958-5036), 3 (3): 11-22 (2002).
Publisher version available at
http://www.liguori.it/periodici.asp?cod_collana=201

NEW MATHEMATICAL MODELS AND CFD NUMERICAL TOOLS FOR THE INVESTIGATION OF MACROMOLECULAR CRYSTAL GROWTH AT MACROSCOPIC AND MICROSCOPIC LENGTH SCALES

Marcello Lappa

Via Salvator Rosa 53, San Giorgio a Cremano, 80046, Napoli, Italy, Fax: +39-81-6042100 and
MARS (Microgravity Advanced Research and Support Center) Via Gianturco 31 - 80146, Napoli, Italy,
Current e-mail address: marcello.lappa@strath.ac.uk, marlappa@unina.it

Abstract - This analysis deals with advances in computational methods for the investigation of macromolecular crystal growth. The modelling of these processes leads to the introduction of a group of equations, strictly related, from a mathematical point of view, to the 'kinetic conditions' used to model mass transfer at the crystal surface as well as to the level of detail required by the analysis ('local' or 'global'); i.e. diversification of the model occurs according to the desired scale length. If the "local" evolution of the crystal surface is the subject of the investigation (distribution of the local growth rate along crystal face, shape instabilities, onset of surface depressions due to diffusive and/or convective effects, etc, i.e. all those factors dealing with the "local" history of the shape) the method must provide "microscopic" and "morphological" details. For this case a 'kinetic-coefficient-based' Volume of Fluid Method is specifically and carefully developed taking into account the possibility of anisotropic (faceted) surface-orientation-dependent growth. On the contrary, if the size of the crystals is negligible with respect to the size of the reactor (i.e. if they are small and undergo only small dimensional changes with respect to the overall dimensions of the cell containing the feeding solution), the shape of the crystals is ignored and the proposed approach relies directly on an algebraic formulation of the nucleation events and on the application of an *integral* form of the mass balance kinetics for each protein crystal. The applicability and the suitability of the different models are discussed according to some worked examples dealing with microgravity conditions.

1. INTRODUCTION

Because of the large size and complexity of protein molecules and the weakness of the bonding forces between them, it is often believed that the experimental principles and methodologies (and associated mathematical models) underlying high-quality inorganic crystal growth are of little help in protein crystallization (Rosenberger [1], McPherson [2]).
Macromolecules are extremely complex physical-chemical systems whose properties vary as a function of many environmental influences. The perplexing difficulties that arise in the crystallization of macromolecules in comparison with conventional small molecules stem from the fact that they are very sensitive to their environment and if exposed to sufficiently severe conditions may denature and/or degrade. Thus common methods for the crystallization of conventional molecules are unsuitable and destructive. They must be supplanted with more gentle and restricted techniques. Because proteins are sensitive and labile macromolecules that readily loose their native structures, the only conditions that can support crystal growth are those that cause little or no perturbation of the molecular properties. For these reasons they are constantly maintained in a thoroughly hydrated state at or near physiological pH and temperature i.e. crystals are grown from a solution to which they are tolerant. This is called the mother liquor. Because complete hydration is essential for the maintenance of structure, protein crystals are always bathed in the aforementioned solvent. The strategy employed to bring about crystallization is to guide the system very "slowly" toward a state of reduced solubility by modifying the properties of the mother liquor.
Since it is expected that growth is driven by the phenomena occurring in a thin zone surrounding the crystal (the so-called "depletion zone", see e.g. [3]) where the concentration of the nutrients is lowered due to solute absorption, many authors have focused on "what happens close to the crystal". Several experimental studies have shown that crystal growth rate is sensitive to very large amount of parameters: e.g. temperature, solution composition, supersaturation, impurities, convection etc. (see e.g. Otàlora and Garcìa-Ruiz [3]). Moreover it usually depends on the crystallographic orientation (Coriell, Chernov, Murray and McFadden [4]) and on crystal habit changes with the level of supersaturation (Pusey, Snyder and Naumann [5], Monaco and Rosenberger [6]). Morphological stability of crystal facets and thus crystal quality also depend on supersaturation and impurities [4]. All these aspects are usually know as "surface kinetics" of the growth process. A comprehensive review of the previous fundamental protein crystal growth and morphology experimental studies has been given for instance in Monaco and Rosenberger [6], Otàlora et al. [7] and

Vekilov and Chernov [8]. A big effort has been made also to understand nucleation kinetics (see e.g. Galkin and Vekilov [9] and references therein).

Macromolecular crystallization is a matter of searching, as systematically as possible, the ranges of the individual parameters that impact upon crystal formation, finding a set or multiple sets of these factors that yield some kind of crystals, and then optimizing the variable sets to obtain the best possible crystals for X-ray analysis.

In light of the arguments given above also “ensemble behaviours” are an important aspect of the problem. In fact, crystallization at a macroscopic scale is characterized by the interplay of different phenomena: transport in liquid phase, nucleation and ensuing growth, competition among different crystals, sedimentation and convection, etc. Understanding of this interplay requires a global analysis that would consider all the relevant phenomena simultaneously in order to track system evolution. Such global analysis may support optimization of growth techniques i.e. it may help to discern interrelations between various "macroscopic" parameters of interest.

To summarize, the crystallization process occurs at two distinct length scales: on the microscopic length scale of the crystal interface, the process is governed by the above-mentioned "surface incorporation kinetics"; and, on the macroscopic scale, the process is controlled by the transport of nutrients available in liquid phase and by the competition for growth of "interacting" crystals ("ensemble behaviours"). In view of the arguments above, the analysis at both microscopic and macroscopic scales plays a crucial role in furthering our knowledge of the overall macromolecular crystal growth.

While efficient numerical methods have been developed and made available for the scientific community in the case of growth of inorganic substances (in particular for the case of crystals grown by thermal solidification of melts under pure diffusive regime or under buoyancy effects, see e.g. Lappa and Savino [10], Voller and Prakash [11], Bennon and Incropera [12]), the modelling of the above-mentioned aspects in the case of growth of protein crystals is still an open task. There is still a disappointing lack of mathematical models and numerical methods able to provide a comprehensive description of the macroscopic ensemble behaviours as well as of all those factors dealing with the "local" history of the crystal surface. Aim of the present paper is to present new mathematical models and tools along these lines.

2. MATHEMATICAL MODEL AND NUMERICAL METHOD

The classical procedure for inducing proteins to separate from solution and produce a solid phase is to gradually increase the level of saturation of a precipitant agent.

Protein precipitants fall into four broad categories: (a) salts; (b) organic solvents; (c) long chain polymers and (d) low-molecular-mass polymers and non-volatile organic compounds.

For a specific protein, the precipitation point (or solubility minima), however, is usually critically dependent on the pH, temperature, the chemical composition of the precipitant and the properties of both the protein and the solvent. Just as proteins may be driven from solution at constant pH and temperature by the addition or removal of salt, they can similarly be crystallized or precipitated at constant ionic strength by changes in pH or temperature.

By these techniques a ‘suitable’ limited degree of supersaturation can be achieved. In very concentrated solutions, in fact, the macromolecules may aggregate as an amorphous precipitate. This result is to be avoided if possible and is indicative that supersaturation has proceeded too extensively or too swiftly.

From a mathematical point of view and in the specific case of mass crystallization from a supersaturated solution one must generally accomplish at least two things simultaneously: (a) determine the concentration fields of organic substance and precipitant in the liquid phase and (b) determine the position of the interface between the solid and liquid phases. According to the technique used to address (a) and (b), in principle the numerical procedures able to solve these problems can be divided into different groups.

If the size of the crystals is negligible with respect to the size of the reactor i.e. if they are small and undergo only small dimensional changes with respect to the overall dimensions of the cell containing the feeding solution, a "macroscopic" approach is required. On the contrary, if the "local" evolution of the crystal surface is the subject of the investigation (distribution of the local growth rate along crystal face, shape instabilities, onset of surface depressions due to diffusive and/or convective effects, etc, i.e. all those factors dealing with the "local" history of the shape) the approach must take into account "microscopic" details.

For the latter case, in principle, transformed co-ordinate systems would be required to account for the position of the crystallization front. This technique for instance has been used by Noh et al. [13]. They investigated the growth behaviours of a precipitate particle in a supersaturated solution under the effect of ‘a priori’ (well-defined) imposed ‘ambient’ flows. The particle was assumed to have initially a spherical shape. The Stokes flow approximation was assumed to simplify the model. Numerical solutions were obtained through numerically generated orthogonal curvilinear co-ordinate system, automatically adjusted to fit the boundary shape at any instant. The initially spherical particle was found to evolve into a peach-like shape if posed in a uniform streaming flow.

This approach to the problem takes the point of view that the interface separating the bulk phases is a mathematical boundary of zero thickness where interfacial conditions are applied. Difficulties arise however when this technique is employed since in this case in the vicinity of the crystallization front (phase change), conditions on mass flux, velocity, and solubility evolution have to be accounted for. This effectively rules out the application of a fixed-grid numerical solution, as deforming grids or transformed co-ordinate systems are required. Moreover the presence of many crystals in the same domain cannot be handled.

On the contrary, a versatile and robust method would require a fixed-grid technique and therefore standard solution procedures for the fluid flow and species equations, without resorting to mathematical manipulations and transformations. This purpose can be obtained by introducing a phase-field variable ϕ which varies in space and time to characterize the phase of the material.

Furthermore, it is worthwhile to stress how this approach leads to "build" methods that can handle the case of microscopic (shape) description as well as the macroscopic behaviour of many interacting crystals. For both cases, the solid mass stored in the generic computational cell can be modelled by assigning an appropriate value of the "phase variable" ϕ to each mesh point (ϕ=1 computational cell filled with solid crystal, ϕ=0 feeding solution and $0<\phi<1$ for a computational cell containing both liquid and solid phases).

Therefore the key element for the method is its technique for adjourning ϕ. Upon changing phase, the ϕ-value of the cell is adjusted to account for mass release or absorption, this adjustment being reflected in the protein (solute) concentration distribution in the liquid phase as either a source or sink. The modelling of these phenomena leads to the introduction of a group of equations, strictly related, from a mathematical point of view, to the 'kinetic conditions' used to model mass transfer at the crystal surface and to the level of detail required by the analysis (macroscopic or microscopic).

From a physical point of view, on a molecular level crystal growth consists of the successive addition of 'growth units' or 'building blocks' to a lattice. Growth units can consist of single molecules or possibly of clusters of molecules. In solution, growth units are typically solvated i.e. are surrounded by highly regularly arranged shells of solvent molecules that interact with the growth unit in a bond-like fashion.

Protein crystallization does not fit any of the traditional (inorganic) models without major modification. The 'attachment rates' in protein crystallization are considerably lower than in most inorganic systems (this slow interface kinetics has been interpreted in terms of the low symmetry and the small binding energies involved in protein crystallization).

Surface attachment kinetics at the crystal surface depend on the local value of solubility and on a coefficient λ (kinetic coefficient) having the dimension of a velocity [cm/s] whose value may be different according to the local orientation of the crystal surface (surface-orientation-dependent growth); using mass balance (see e.g. Rosenberger [1] and Pusey et al. [5]), and assuming a linear dependence of the growth rate by the interface supersaturation (see e.g. Lin et al. [14] and Lappa [15]), one obtains:

$$\left(\frac{D}{\rho_P - \rho_C C_{cs}/\rho_L}\right)\left.\frac{\partial C}{\partial n}\right|_{cs} = \lambda(\underline{\hat{n}})\left(\frac{C_{cs}-S}{S}\right) \qquad (1)$$

where C_{cs} is the concentration of the protein at the crystal surface, D is the related diffusion coefficient, S is the solubility (its value is function of the local concentration of the precipitant agent and/or of temperature), ρ_P and ρ_C are the protein mass density and the total mass density in the crystal, ρ_L is the total density of the solution, λ is the kinetic coefficient and $\underline{\hat{n}}$ is the unit vector perpendicular to the crystal surface pointing into the liquid. The dependence on $\underline{\hat{n}}$ takes into account anisotropic growth. This situation occurs for crystalline proteins which have high anisotropy (preferred orientations) in either their surface energy or atomic attachment kinetics.

Whenever protein in solute phase and solid crystal co-exist in equilibrium (saturation condition):

$$C_{cs} = S \qquad (2)$$

In a saturated solution, two states exist in equilibrium, the solid phase, and one consisting of molecules free in solution. At saturation, no net increase in the proportion of solid phase can accrue since it would be counterbalanced by an equivalent dissolution. Thus 'crystals do not grow from a saturated solution'. The system must be in a non-equilibrium, or supersaturated state to provide the thermodynamic driving force for crystallization (McPherson [2]).

Solution must by some means be transformed or brought into the supersaturation state whereby its return to equilibrium, forces exclusion of solute molecules into the solid state, the crystal. As long as C_{cs} <S, more solid material will dissolve if any. If, on the other hand, C_{cs} >S, material will condense on any material *already existing* and augment its size. The solution is said to be *supersaturated* when the solute content is greater than S, and the degree of supersaturation σ is defined by σ =C/S.

At this stage, diversification of the model is needed according to the desired scale length. The mathematical conditions accounting for the surface kinetics in fact behave as *differential* equations in the case of microscopic approach and as *integral* balance laws if the analysis is carried out at macroscopic scale (investigation of the "ensemble behaviour").

2.1 MACROSCOPIC ANALYSIS AND INTEGRAL FORMULATION OF THE KINETIC CONDITIONS

If the shape of the crystal and its morphological time-evolution are not an essential part of the problem, the mathematical approach can rely directly on the application of an *integral* form of the kinetic balance law for each protein crystal. The shape of the crystals is ignored. Each solid particle is considered in terms of its mass and position within the reactor. Accordingly, to account for the kinetic condition, eq. (1) is re-written as an integral condition to be applied along the frontier $\partial\Omega$ of the computational cell containing the solid particle. The concentration at the crystal surface (C_{cs}) is assumed to be equal to the value of the concentration C computed along the frontier of the computational cell containing the crystal. Of course C_{cs} is not constant along the frontier; it has a different value according to the side where it is computed i.e. the integral form of eq. (1) takes into account the relative direction of the different

faces, which induces varying conditions for each face. In particular, for each face C_{cs} is expressed as average value ($C_i^{average}$) with respect to the concentration $\widetilde{C}$ of the cell accommodating the crystal and that of the neighbour cell sharing the face in question $C_i^{neighbour}$.

Integrating over the frontier of the computational cell equation (1) reads:

$$\int_{\partial\Omega} D\ \underline{\nabla} C\cdot\underline{\hat{n}}\ dA=\int_{\partial\Omega}\lambda\left(\rho_P-\rho_C\frac{C_{cs}}{\rho_L}\right)\left(\frac{C_{cs}}{S}-1\right)dA \qquad (3)$$

now $\underline{\hat{n}}$ is the unit vector perpendicular to the computational cell frontier pointing into the generic neighbour cell. In discretized form:

$$\sum_i D\ \left.\frac{C_i^{neighbour}-\widetilde{C}}{\Delta n}\right|_i A_i = \sum_i \lambda\left(\rho_P-\rho_C\frac{C_i^{neighbour}+\widetilde{C}}{2\rho_L}\right)\left(\frac{C_i^{neighbour}+\widetilde{C}}{2S}-1\right)A_i \qquad (4)$$

The concentration $\widetilde{C}$ satisfying the integral form of eq. (1) is obtained from eq. (4), then the mass stored in the computational cell is updated according to the equation:

$$\frac{\partial M}{\partial t}=\int_{\partial\Omega}\lambda\left(\rho_P-\rho_C\frac{C_{cs}}{\rho_L}\right)\left(\frac{C_{cs}}{S}-1\right)dA\rightarrow$$

$$\frac{\partial\phi}{\partial t}=\frac{1}{\Delta v}\int_{\partial\Omega}\lambda\left(1-\frac{\rho_C}{\rho_P}\frac{C_{cs}}{\rho_L}\right)\left(\frac{C_{cs}}{S}-1\right)dA \qquad (5)$$

The volume [cm^3] of the crystal mass M stored in a grid cell in fact can be computed as:

$$dv\big|_{stored}=\frac{M}{\rho_P}\rightarrow\ \phi=\frac{dv|_{stored}}{dv} \qquad (6)$$

where ρ_P is the protein mass density in the crystal and dv is the volume of the computational cell. Hence (n superscript denotes time step):

$$\phi^{n+1}=\phi^n+\Delta t\cdot\frac{1}{\Delta v}\sum_i\lambda\left(1-\frac{\rho_C}{\rho_P}\frac{C_i^{neighbour}+\widetilde{C}}{2\rho_L}\right)\left(\frac{C_i^{neighbour}+\widetilde{C}}{2S}-1\right)A_i \qquad (7)$$

with $\widetilde{C}$ satisfying eqs. (4).

According to equations (4) and (7) the growth velocity is not directly imposed but it results from internal conditions related to solute transport and incorporation kinetics. If the protein (solute) concentration is locally depleted, correspondingly, the solid mass stored in the computational cell grows and the phase variable is increased; on the other hand if mass stored in the cell begins to re-dissolve, protein is released in solute phase and the local value of protein concentration is increased.

The shape of the crystals is ignored while sacrificing little in accuracy for the macroscopic description of the spatio-temporal behaviour. Evidence of the reliability of the present assumptions is provided by the good agreement between experimental and numerical results (see e.g. Lappa, Piccolo and Carotenuto [16]) as will be shown in the next section.

It is worthwhile to stress how the technique discussed above for the case of crystals modelled only in terms of mass and position, allows a simple and efficient treatment of the nucleation phenomena.

When there is no pre-existing deposit, it is generally found that the concentration of protein has to be greater than S to create one spontaneously, say

$$\sigma\geq\eta \qquad (8)$$

where η is the supersaturation limit ($\eta>1$); once nuclei are created, precipitation can continue if $1<\sigma\leq\eta$ and vice-versa material can come back to the solute condition if $0<\sigma<1$. Further details on the well known physics of these phenomena can be found in the excellent theoretical analysis of McPherson [2]. According to the crystallization criteria introduced by Henisch and Garcìa Ruiz [17] and Henisch [18] (algebraic model), once the solid particles are formed it is assumed that they are in equilibrium with protein and salt in liquid phase. This assumption is supported by the well-known fact that "at the supersaturation required for nucleation, crystals typically grow extremely rapid" (Galkin and Vekilov [9]). If the supersaturation limit is exceeded, the amount of supersaturated protein in liquid phase is posed in solid without any time delay (Lappa and Castagnolo [19], Lappa, Castagnolo and Carotenuto [20], Lappa and Carotenuto [21]). Thus the solute content of the solution will have to be decremented from the original C value to the solubility value.

If $\phi^n=0$ and $\sigma^n=(C/S)^n\geq\eta\rightarrow$

$M_{grain(o)}=\left(C-S\right)^n\Delta v$,

$$\phi^{n+1}=\frac{1}{\Delta v}\frac{M_{grain(o)}}{\rho_P}=\frac{S^n}{\rho_P}\left(\sigma^n-1\right),\quad C^{n+1}=S^n \qquad (9)$$

This nucleation model has been also successfully used by Piccolo et al. [22] and Carotenuto et al. [23] to elucidate their experimental results.

2.2 MICROSCOPIC ANALYSIS AND DIFFERENTIAL FORMULATION OF THE KINETIC CONDITIONS

If a detailed description of the local evolution of the crystal is required (distribution of the local growth rate along crystal face, growth habit simulation, onset of surface protuberances due to diffusive and/or convective effects, etc), the surface attachment kinetic conditions are used to introduce a group of differential equations for the protein concentration at the crystal surface and the evolution of the solid mass displacement.

In this case the crystals are no longer modelled as "single" computational cells. Each crystal occupies a significant portion (i.e. a large number of computational cells) of the computational domain and protein concentration must satisfy the differential kinetic condition (1) along its surface ($\left|\underline{\nabla}\phi\right|\neq 0$,$0<\phi<1$):

$$\underline{\hat{n}} = -\frac{\underline{\nabla\phi}}{|\underline{\nabla\phi}|} = (\alpha, \beta) \tag{10}$$

$$\alpha = -\frac{\partial\phi}{\partial x} \Big/ \sqrt{\left(\frac{\partial\phi}{\partial x}\right)^2 + \left(\frac{\partial\phi}{\partial y}\right)^2}$$

$$\beta = -\frac{\partial\phi}{\partial y} \Big/ \sqrt{\left(\frac{\partial\phi}{\partial x}\right)^2 + \left(\frac{\partial\phi}{\partial y}\right)^2} \tag{11}$$

since $\frac{\partial C}{\partial n} = \alpha\frac{\partial C}{\partial x} + \beta\frac{\partial C}{\partial y}$, (hereafter the subscript 'cs' is omitted) eq. (1) can be written as

$$\alpha\frac{\partial C}{\partial x} + \beta\frac{\partial C}{\partial y} = \frac{\lambda}{D}(\alpha, \beta)(\rho_P - \rho_C C/\rho_L)(C/S - 1) \tag{12}$$

$\lambda(\rho_P - \rho_C C/\rho_L)(C/S-1)$ represents the mass exchange flux between solid and liquid phase (i.e. crystal and protein solution). The mass stored in computational cells that are undergoing phase change can be computed according to the equation:

$$\frac{\partial M}{\partial t} = \lambda(\alpha, \beta)(\rho_P - \rho_C C/\rho_L)(C/S - 1)ds \tag{13}$$

where ds is the 'reconstructed' portion of the crystal surface (by definition perpendicular to the interface normal vector $\underline{\hat{n}}$) 'bounded' by the frontier of the control volume (computational cell) located astride the crystal surface. Therefore the phase field equation reads

$$\frac{\partial\phi}{\partial t} = 0, \text{ if } |\underline{\nabla\phi}| = 0$$

$$\frac{\partial\phi}{\partial t} = \frac{\lambda(\alpha, \beta)(\rho_P - \rho_C C_{cs}/\rho_L)(C_{cs}/S - 1)ds}{\rho_P dv}$$

$$\text{if } |\underline{\nabla\phi}| \neq 0,\ 0<\phi<1 \tag{14}$$

with C satisfying eq. (10).

Equations (12), (13) and (14) behave as 'moving boundary conditions', their solution being strictly associated to the computational check on the value of ϕ and its gradient.

In practise, the unit vector $\underline{\hat{n}}$ results from the gradient of a smoothed phase field $\widehat{\phi}$, where the transition from one phase to the other takes place continuously over several cells (4 or 5). The smoothed phase field $\widehat{\phi}$ is obtained by convolution of the unsmoothed field ϕ with an interpolation function.

Depending on the interface's orientation, concentration gradients are discretized by forward or backward schemes. For this reason eq. (12) in discretized form reads:

$\alpha>0, \beta>0$: (15a)

$$C_{i,j}^{n+1} = \frac{\left[(\lambda/D)(\rho_P - \rho_C C_{i,j}^{n+1}/\rho_L) + \alpha\ C_{i+1,j}^{n+1}/\Delta x + \beta\ C_{i,j+1}^{n+1}/\Delta y\right]}{\left[(\lambda/D)(\rho_P - \rho_C C_{i,j}^{n+1}/\rho_L)/S + \alpha/\Delta x + \beta/\Delta y\right]}$$

(15b)

$\alpha<0, \beta>0$: (15b)

$$C_{i,j}^{n+1} = \frac{\left[(\lambda/D)(\rho_P - \rho_C C_{i,j}^{n+1}/\rho_L) - \alpha\ C_{i-1,j}^{n+1}/\Delta x + \beta\ C_{i,j+1}^{n+1}/\Delta y\right]}{\left[(\lambda/D)(\rho_P - \rho_C C_{i,j}^{n+1}/\rho_L)/S - \alpha/\Delta x + \beta/\Delta y\right]}$$

(15b)

$\alpha>0, \beta<0$: (15c)

$$C_{i,j}^{n+1} = \frac{\left[(\lambda/D)(\rho_P - \rho_C C_{i,j}^{n+1}/\rho_L) + \alpha\ C_{i+1,j}^{n+1}/\Delta x - \beta\ C_{i,j-1}^{n+1}/\Delta y\right]}{\left[(\lambda/D)(\rho_P - \rho_C C_{i,j}^{n+1}/\rho_L)/S + \alpha/\Delta x - \beta/\Delta y\right]}$$

(15c)

$\alpha<0, \beta<0$: (15d)

$$C_{i,j}^{n+1} = \frac{\left[(\lambda/D)(\rho_P - \rho_C C_{i,j}^{n+1}/\rho_L) - \alpha\ C_{i-1,j}^{n+1}/\Delta x - \beta\ C_{i,j-1}^{n+1}/\Delta y\right]}{\left[(\lambda/D)(\rho_P - \rho_C C_{i,j}^{n+1}/\rho_L)/S - \alpha/\Delta x - \beta/\Delta y\right]}$$

$C_{i,j}^{n+1}$ is computed from equation (15) iterating up to reach convergence, then the phase variable is updated using equation (14):

$$\phi_{i,j}^{n+1} = \phi_{i,j}^{n} + \Delta t\frac{\lambda(\rho_P - \rho_C C_{i,j}^{n+1}/\rho_L)(C_{i,j}^{n+1}/S - 1)\Delta s}{\rho_P \Delta x \Delta y} \tag{16}$$

According to equations (15) and (16), the phenomena are driven by the attachment kinetic condition, i.e. the existing deposit grows if protein concentration is larger than S and the mass exchange is proportional to the local value of the orientation-dependent kinetic coefficient; in the opposite situation, i.e. in case protein concentration becomes smaller than S, deposit begins to re-dissolve.

In eq. (16) Δs is the 'reconstructed' portion of the solid wall 'bounded' by the frontier of the control volume (computational cell) located astride the crystal surface. The determination of Δs requires a well defined 'interface-reconstruction' technique (the shape of the crystal for a fixed time is not known a priori and must be determined as part of the solution). A reconstruction is a geometrical approximation of the true solid/liquid interface. Usually the interface can be approximated by a straight line of appropriate inclination in each cell. Various conditions can be used to determine the reconstruction, one of which is a condition that the straight lines connect at cell-faces. With this condition, the resulting interface representation becomes continuous. However, for strong distortions and topology changes similar to those involved in organic crystal growth, this conditions becomes virtually unenforceable. If non-connecting straight lines (each line is determined independently of the neighbour lines and their ends need not necessarily connect at the cell-faces, see e.g. Gueyffier et al. [24]) are used, this guarantees maximum robustness and simplicity, and allows extension to three dimensions, while sacrificing little in accuracy.

Two conditions have to be used for the straight line in cell (i,j), which always yield an unambiguous solution: a) it is perpendicular to the interface-normal-unit vector $\underline{\hat{n}}$; b) it delimits a solid area 'matching' the given $\phi_{i,j}^{n}$ for the cell.

The present technique shares with the classical VOF methods the interface orientation analysis, that in these methods is needed to compute the surface tension force

perpendicular to the interface separating the fluid-phases (expressed as a corresponding volume force, which can be included in the momentum equation), whereas here it is needed for the orientation-dependent kinetic coefficients and the discretization of the protein concentration gradients perpendicular to the surface.

2.3 GOVERNING FIELD EQUATIONS

The mass transport in the liquid phase surrounding the solid mass is governed by the continuity, Navier-Stokes and species equations, that in conservative form read :

$$\underline{\nabla} \cdot \underline{V} = 0 \tag{17}$$

$$\frac{\partial \underline{V}}{\partial t} = -\frac{1}{\rho}\underline{\nabla} p - \underline{\nabla} \cdot [\underline{V}\underline{V}] + \upsilon \nabla^2 \underline{V} \tag{18}$$

$$+ g\beta_{protein}\left(C - C_{(o)}\right)\underline{i}_g + g\beta_{NaCl}\left(C_{NaCl} - C_{NaCl(o)}\right)\underline{i}_g - \frac{1}{\chi}\underline{V}$$

$$\frac{\partial C}{\partial t} = (1-\phi)\left[-\underline{\nabla} \cdot (\underline{V}C) + D\,\nabla^2 C\right] \tag{19}$$

$$\frac{\partial C_{salt}}{\partial t} = (1-\phi)\left[-\underline{\nabla} \cdot (\underline{V}C_{salt}) + D_{salt}\nabla^2 C_{salt}\right] \tag{20}$$

where ν is the kinematic viscosity, V and p are the velocity and pressure and $C_{(o)}$ and $C_{salt(o)}$ are the initial value of protein and precipitant agent (salt) respectively. The Boussinesque approximation is used to model the buoyancy forces: $\beta_{protein}$ and β_{salt} are the solutal expansion coefficients related to organic substance and salt respectively. Note that in case solubility modulation is induced by temperature control, eq. (20) must be replaced by the energy equation.

Assumptions invoked in the development of equations for this continuum model include: laminar flow, Newtonian behaviour of the phases (this implies that solids, should be treated as highly viscous fluids), constant phase densities (and Boussinesque approximation).

Moreover the solid phase (crystal) is assumed to be nondeforming and free of internal stress, while the multiphase region (region where phase change occurs) is viewed as a porous solid characterized by an isotropic permeability χ by analogy with the enthalpy methods (see, e.g., Lappa and Savino [10], Voller and Prakash [11], Bennon and Incropera [12]).

The species equations (19) and (20) are solved throughout the computational domain including both the solid and liquid phases. The presence of the term (1-ϕ) ensures in fact that the solid phase is impermeable to protein and precipitant in solute phase.

An important problem with fixed-grid solution procedures, is accommodating the zero velocity condition, which is required as a liquid region turns to solid. Various methods can be used in principle to 'switch off' velocities in computational cells that are becoming solid (or 'switch on' velocities in the reverse case). Velocities may simply be set to zero. Another possible approach is based on the viscosity. The viscosity of a cell is driven to a very large value as the solid mass stored in this cell increases. The increasing viscosity provides the necessary coupling between the physical state of the material in the cell and the momentum equations, thereby driving velocities to zero in cells that are solid. A third possible approach (porosity approach) requires that computational cells that are undergoing a phase change are modelled as a pseudo-porous media, with the porosity χ being a function of ϕ ranging between 0 (fully liquid cell) and 1 (fully solid cell). For the present case of macromolecular organic crystal growth, this assumption is based directly on the fact that solid formation occurs as a 'permeable' crystalline matrix which coexists with the liquid phase. The term $-\underline{V}/\chi$ in equation (18) is the Darcy term added to the momentum equation to eliminate convection in the solid phase. In the present analysis permeability is assumed to vary according to the Carman-Kozeny equation (Bennon and Incropera [12]).

$$\chi \propto \frac{(1-\phi)^3}{\phi^2} \tag{21}$$

In the pure solid (ϕ=1) and pure liquid (ϕ=0), equation (21) reduces to the appropriate limits, namely χ=0 and χ = ∞ respectively. In practice the effect of χ is as follows: in full liquid elements 1/χ is zero and has no influence; in elements that are changing phase, the value of χ will dominate over the transient, convective and diffusive components of the momentum equation, thereby forcing them to imitate Carman-Kozeny law; in totally solid elements, the final large value of 1/χ will swamp out all terms in the governing equations and force any velocity predictions effectively to zero.

Since the momentum equation is valid throughout the entire domain, explicit consideration need not be given to boundaries between solid, multiphase and liquid regions.

3. RESULTS AND EXAMPLES

In order to shed further light on the techniques described in section 2.1 and 2.2 and in particular on the related field of applications, in the present section, some "reference" cases are discussed and elucidated. Such discussion may help the Reader in discerning both the advantages and limitations of the microscopic and macroscopic approaches respectively.

Hen egg white lysozyme is used as model protein, being a well-characterised and widely-used molecule (see Table 1 for the properties). The precipitant agent is NaCl. Two 'typical' cases are considered. In the first case (Figs. 1-4), the growth of a lysozyme seed (size 1 [mm]) is investigated under the effect of buoyancy convection induced by typical values of residual gravity occurring on orbiting space platforms (e.g., the Space Shuttle or the International Space Station). In the second case (Figs.5-7), the formation of a multi-crystal pattern is investigated in the framework of a counter-diffusion technique and zero-g conditions.

The microscopic approach is essential for the correct simulation of all those situations dealing with the case of only one or few crystals simultaneously growing in the protein reactor. Often crystal growers in fact are

interested to investigate "local" aspects of the growth e.g. growth depending on the crystallographic orientation, crystal habit changes with the level of supersaturation (growth habit simulation and microscopic facet morphology study), onset of surface depressions or protuberances due to convective effects, etc.

Here, as anticipated, the growth of a seed of lysozyme under micro-gravity conditions ($g=10^{-4}\ g_O$) is simulated. For the sake of simplicity (aim of the present paper is merely to show the capabilities of the numerical method and how it can 'capture' heretofore poorly understood physics and mechanics of the problem under investigation) the initial shape of the seed is supposed to be quadrate and the kinetic coefficient is supposed to be the same for the different sides of the crystal (however the numerical method can handle complex shapes and surface-orientation-dependent growth as shown in paragraph 2.2).

The seed (1 [mm] x 1 [mm]) is supposed to be fixed (e.g. by glue) to the mean point of the left wall of the reactor (10 [mm] high and 30 [mm] wide test cell) used for the growth process (see figure 3). Growth is obtained from a super-saturated solution with $C_{lys(o)}=5\cdot10^{-2}$ [g cm^{-3}] and $C_{NaCl(o)}=2.5\cdot10^{-2}$ [g cm^{-3}] ($\sigma_{(o)}\cong5$). These conditions guarantee growth of the existing single seed and absence of new nucleation phenomena. The frontier of the domain is supposed to be impermeable to the protein.

If the presence of convection is taken into account a flow field is driven by the density gradient around the growing crystal. Since isothermal conditions are assumed throughout the growth process, only compositional nonuniformities, that evolve in the solution due to the crystallization process, act as source for buoyancy-driven convection. This flow field modifies the protein distribution around the crystal leading to a non-symmetrical concentration pattern (fig. 3). One recognizes the well-known convective flow pattern for solution growth with a rising 'plume' above the crystal. When growth sets in, the solute concentration around the crystal seed decreases. With this depletion of the heavier solute, the solution around the crystal becomes lighter and, thus, rises.

From a 'local' point of view, the simulations show that corners and edges of the crystal are more readily supplied with solute than the centre of faces (this leads to a macroscopic depression around the centre of the faces, see figure 1 and figure 3). This is due to the pattern of the protein concentration field around the crystal. Incorporation of the solute into the crystal causes a local depletion in concentration and a solutal concentration gradient to form between the bulk solution and the growth interface. The 'steepness' of the gradient determines the rate of solute transport to the growth interface, the steepness being maximum around the corners. Superimposed on this is the fact that a protuberance on the interface sees a higher supersaturation and grows faster than a depression, which sees a lower supersaturation. Note that the existence of 'depressions' around the centre of the faces of growing crystals (shown by the present numerical results) has been often observed experimentally (Monaco and Rosenberger [6]). Figure 1 shows that the difference in gradient steepness between face corner and face centre (and consequently the 'depth' of the depressions) is proportional to the size of the crystal.

Figure 2b shows in particular that the 'face' (average) growth rate exhibits a different value according to the orientation of the face with respect to the direction of the residual g.

This clearly demonstrates that orientation-dependent growth may occur even if the dependence of the kinetic coefficients on the orientation of the faces is neglected. In this case, it is due to the non-symmetrical concentration pattern around the crystal distorted by the effect of convection according to the direction of the residual g. The growth rate is strongly affected by the mass transport in liquid phase and g-orientation-dependent growth occurs.

Figure 1 shows that the increase of volume of the crystal is more pronounced for the bottom side than for the upper side. Figure 2b and 4 show in detail how the convection effect results in higher local growth rates near the surface where the flow is incoming and lower local growth rates near the surface where the flow is outgoing. This behaviour can be explained according to two different effects.

Due to the convective structure of the flow pattern, in fact, liquid is transported towards the bottom side and in opposite direction around the upper side. According to this behaviour, liquid regions where the amount of protein available in liquid phase is still large are transported towards the bottom side of the crystal. This increases the growth rate of the lower face (a large amount of protein in solute phase is available for crystal growth). On the other hand, due to the outgoing flow, the depletion zone close to the upper face is distorted and elongated towards the top of the test cell ('plume'). This leads to a decrease of the concentration gradient (the depletion layer becomes thicker with respect to the bottom side of the crystal) and hence to a decrease of the mass exchange flux between solid and liquid phase. This explains the occurrence of a higher value of the growth rate on the bottom face.

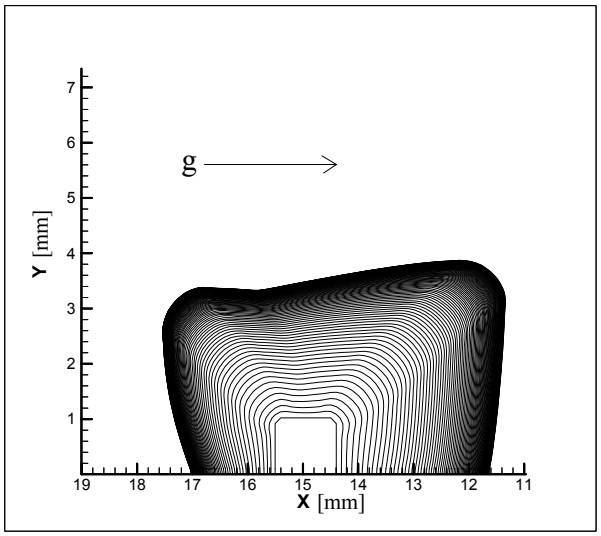

Fig.1: Growth habit simulation of a single seed of lysozyme ($C_{lys(o)}=5\cdot10^{-2}$ [g cm^{-3}], $C_{NaCl(o)}=2.5\cdot10^{-2}$ [g cm^{-3}]): microgravity convective conditions, snapshots of the crystal shape versus time ($\Delta t= 3.5\ 10^4$ [s]).

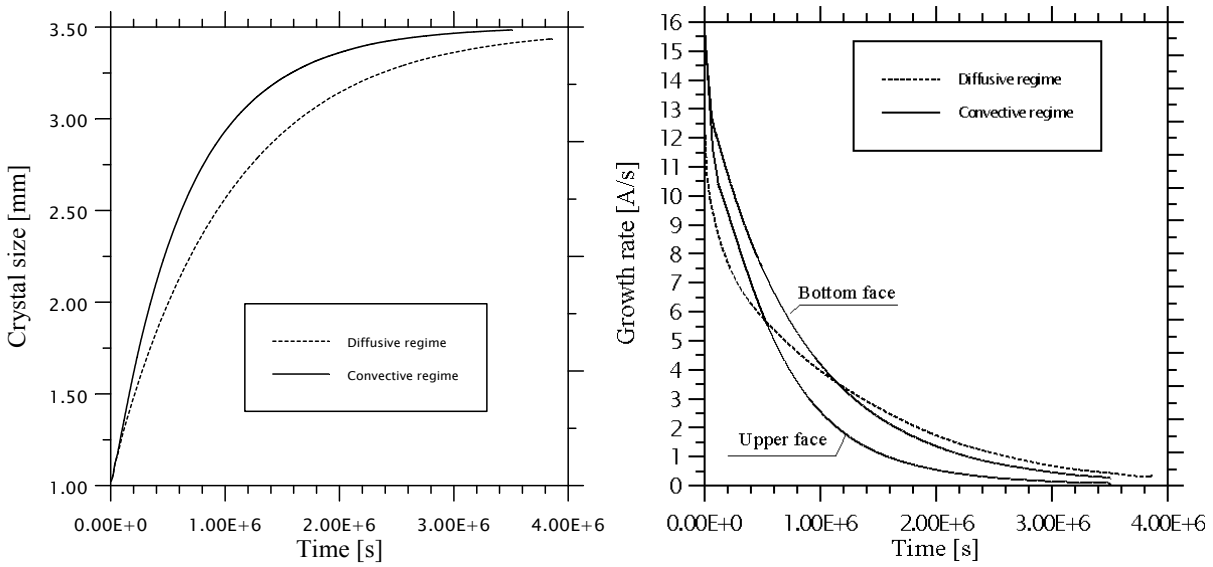

Fig. 2: isothermal protein crystal growth system under diffusive and microgravity (convective) conditions (single crystal of initial dimensions 1 [mm] x 1 [mm] fixed to the left wall of a 3 [cm] high and 1 [cm] wide growth cell; $C_{lys(o)}=5\cdot10^{-2}$ [g cm^{-3}] and $C_{NaCl(o)}=2.5\cdot10^{-2}$ [g cm^{-3}]): (a) average size (along y) versus time; (b) growth rate versus time.

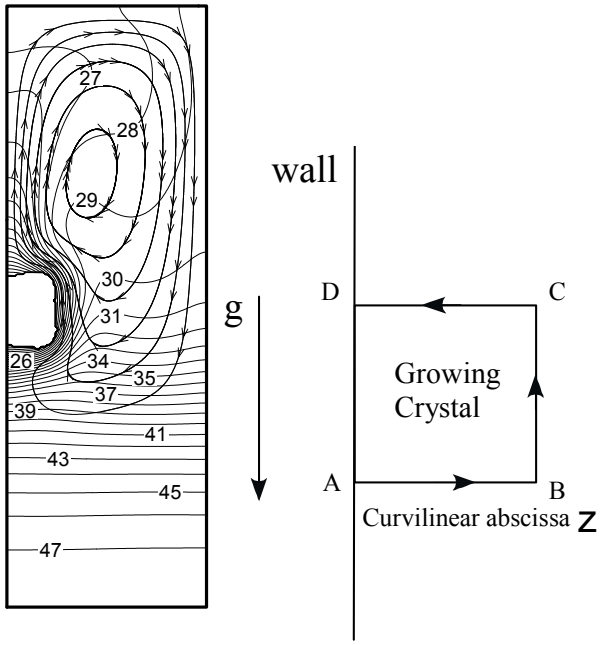

Fig.3: Snapshot of growing crystal, concentration distribution and velocity field under microgravity conditions (g=10^{-4} go; level 1→C=$2.9\cdot10^{-2}$, level 50→C=$5.0\cdot10^{-2}$, ΔC≅$4.3\cdot10^{-4}$)

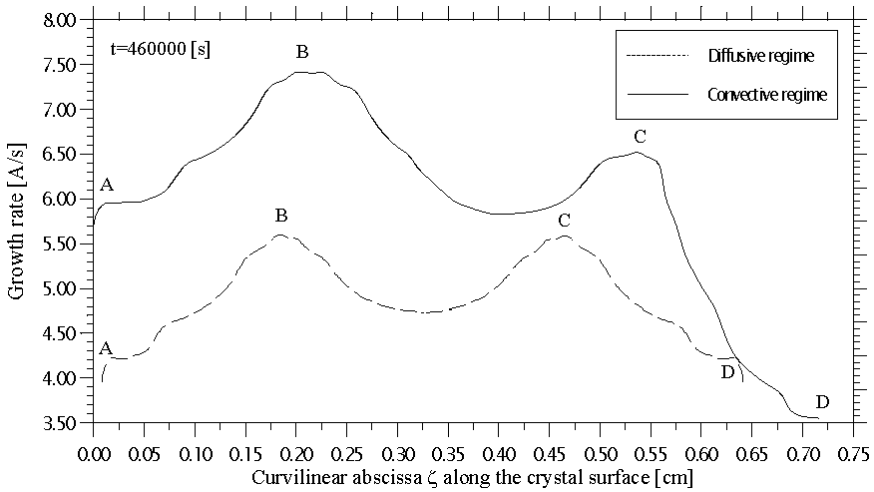

Fig.4: Surface growth rate distribution under diffusive and microgravity (convective) conditions.

If the problem under investigation is characterized by the formation of new crystals and by multiple nucleation phenomena, the morphology-oriented method described above is no longer suitable for a comprehensive analysis of the system. For instance this occurs in the case of crystal grown by a counter-diffusion technique. In this case: a) the nucleation and growth phenomena self-limit maximal supersaturation that is actually reached during the crystallization, thus establishing better conditions for obtaining relatively large single crystals; b) a range of supersaturations is established in different locations along the protein solution during the process leading to different crystallization conditions in the same experiment.

The case of a gellified protein chamber is considered (this condition is equivalent to zero-g). This chamber is put in contact with an additional chamber containing the precipitant agent (salt). Therefore the configuration under investigation simply consists of a protein solution and a precipitant agent solution placed one above the other and separated by the gel interface. The crystallization cell is a chamber whose length and height are L and H respectively; the interface is placed at $y \cong h$. At the initial time, both solutions are at constant concentration respectively. As time passes salt diffuses in the protein chamber through the gel interface lowering the solubility and starting nucleation and ensuing growth phenomena.

The following properties and operating conditions have been used for the numerical simulations: $C_{NaCl(o)} = 14 \cdot 10^{-2}$ [g cm^{-3}], L = 1 [cm], H = 4 [cm], width = 0.1 [cm], average height of the protein chamber h = 1.95 [cm].

Simulations show that some "bands" of crystals are produced in the gel .i.e. discrete nucleation events separated by certain time (and thus space) intervals occur in the protein chamber. These bands are not spatially uniform (see Figs. 6; note that in these figures the salt chamber is located on the top of the protein chamber). According to the evolution of the protein concentration field (Figs.5) nucleating particles deplete their surroundings of protein which causes a drop in the local level of supersaturation such that the nucleation rate falls in the neighbourhood, leading naturally to a spacing between regions of nucleation that gives rise to the alternate presence of depleted zones and crystals. This behaviour exhibits interesting analogies with the well-known so-called "Liesegang patterns" (see e.g., Henisch and Garcìa-Ruiz [17] and Lappa et al. [20]).

The spacing among different solid particles and the size of the particles seem to vary according to the distance from the origin of the imposed concentration gradient (for the present case the gel interface between the salt and protein chambers). The space distance among near solid particles, in fact, tends to decrease uniformly towards the interface of the protein chamber. Correspondingly the size of these particles is minimum at the interface and increases towards the bottom of the chamber up to a constant value in the bulk. According to the results discussed above, the “density of particles” defined as ratio of the number of particles in a fixed reference volume and the reference volume, is maximum near the interface and almost constant in the bulk. These behaviours are shown in Figs. 7.

The proposed models and methods exhibit heretofore unseen capabilities to predict and elucidate experimental observations at macroscopic level and to identify cause-and-effect relationships. Both experimental observation and numerical modelling show comparable features of the phenomena under investigation. The consistency of model predictions with experimental data suggests that the proper rate-controlling steps have been taken into account, and that simplifications do not influence much the system behaviour.

Though the model is oriented to the description of macroscopic behaviours, however it is also able to provide some interesting information dealing with the crystal growth as a function of local conditions established in the protein chamber. As an example Fig. 7c shows the growth law for a reference crystal located in the bulk of the protein chamber (x =0.4 [cm], y=0.9 [cm]); the growth is compared with the evolution of local supersaturation. This crystal is formed at $t \cong 7 \cdot 10^4$ [s] and reaches its final size after almost 10^5 seconds. A "measure" of the average growth rate is also possible. The growth rate (computed over the time interval required to reach the 90% of the final mass of the crystal) is 1.27 10^{-9} [g/s]. As previously pointed out, however, the shape of the crystal is ignored and for this reason only an "integral" growth rate (accounting for the total mass variation) can be computed for each crystal.

In view of the above arguments the macroscopic approach has proven to be a very efficient and robust method to be used when a very large number of interacting crystals is involved in the growth process (this situation often occurs in the case of the aforementioned counter-diffusion techniques). In this case the model predicts the main features of the process, providing spatial and size distributions of crystals that are in good agreement with the experimental observations and very interesting information about the "ensemble behaviour".

It important to point out that a local detailed description of the morphology evolution of all the particles in Figs. 6 according to the method elucidated in section 2.2 would require very dense grids (of the order of 10^7 points) and therefore a prohibitive computational time.

4. CONCLUSIONS AND DISCUSSION

Some powerful and original mathematical tools have been made available for the scientific community to help the investigators to simulate their experiments at macroscopic and microscopic length scales.

A more comprehensive method should introduce a bi-level grid, and use a macro-grid on the scale of the process for the solution of equations describing macroscopic mass transport and a micro-grid on which equations describing the microscopic phenomena for each crystal (if many) are solved. In this way, a dual-scale model would be obtained able to capture both the macro and micro-scales in a single numerical treatment. This objective is delayed to a forthcoming paper.

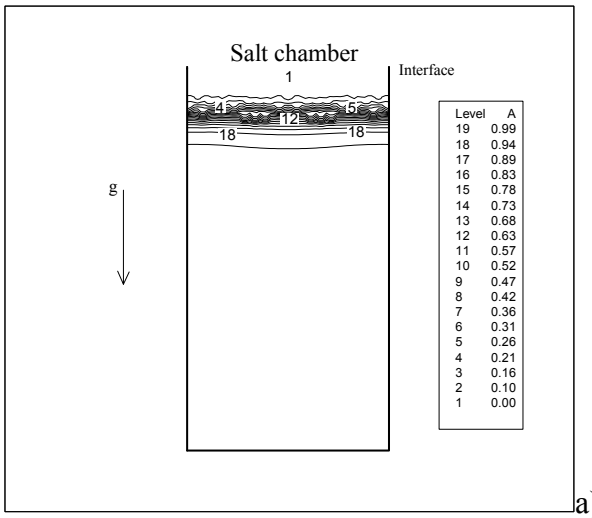

a)

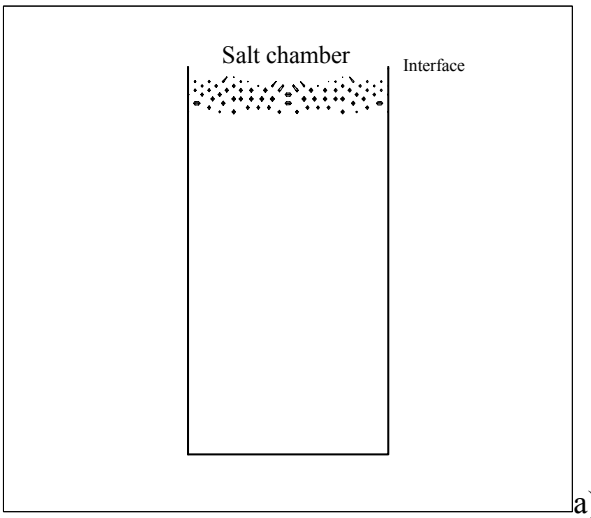

a)

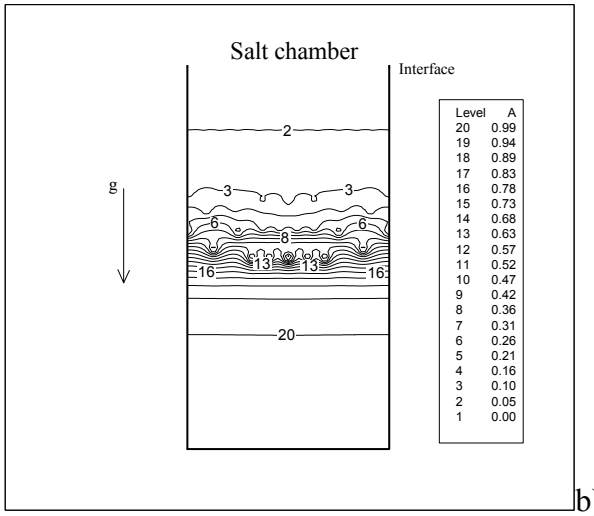

b)

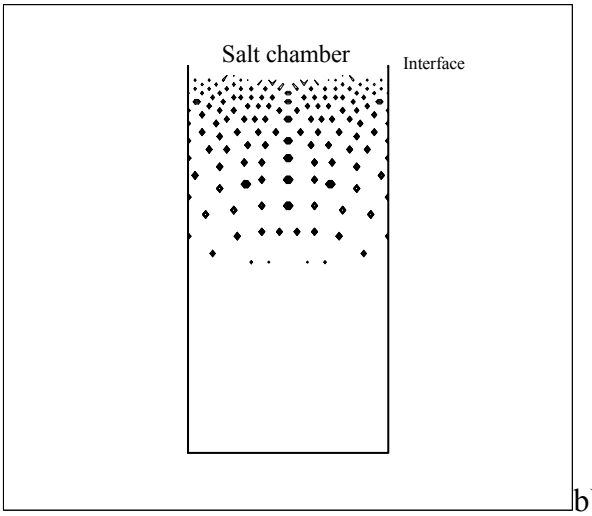

b)

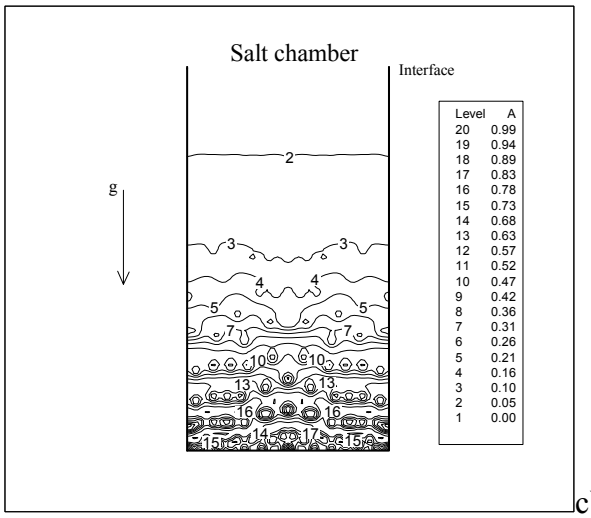

c)

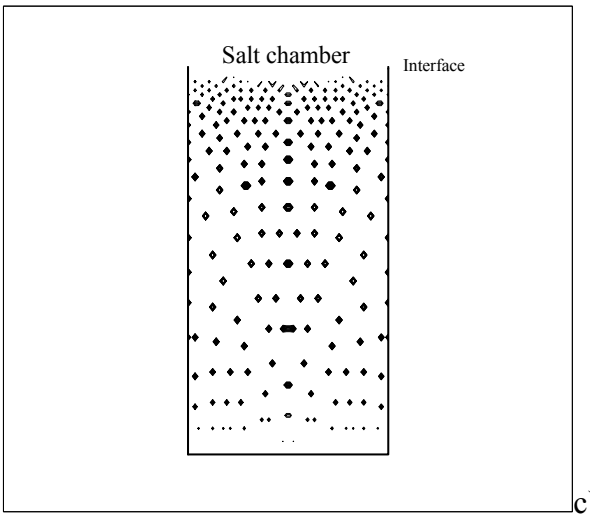

c)

Figs. 5 Figs. 6

Non-dimensional protein concentration contour lines (Figs. 5) and distribution of the crystals (Figs. 6)–(zero-g conditions, $C_{(o)} = 4 \cdot 10^{-2}$ [g cm^{-3}]) Time=$8.00 \cdot 10^3$ [s], $7.2 \cdot 10^4$ [s], $1.08 \cdot 10^5$ [s].

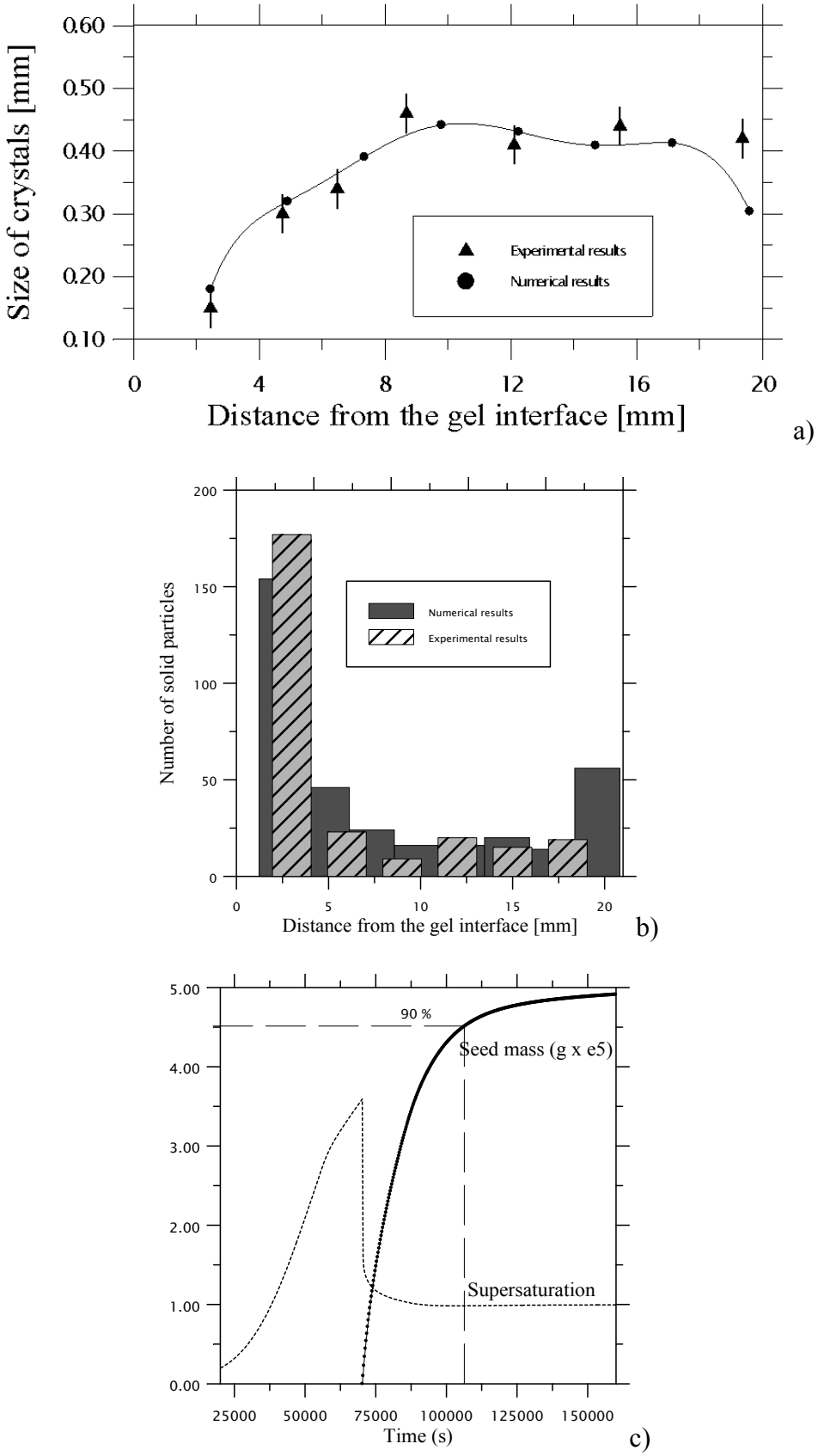

Figs.7: comparison between numerical and experimental results (gellified configuration, $C_{(o)} = 4 \cdot 10^{-2}$ [g cm^{-3}]): (a) solid particle size distribution, (b) density of particles distribution, (c) computed "growth law" of a reference crystal (x = 0.4 [cm], y=0.9 [cm]) located in the bulk of the protein chamber.

D_{lys} [cm^2 s^{-1}]	10^{-6}
D_{NaCl} [cm^2 s^{-1}]	10^{-5}
ν [cm^2 s^{-1}]	$8.63 \cdot 10^{-3}$
ρ_c [g cm^{-3}]	1.2
β_{lys} [g^{-1} cm^3]	0.3
β_{NaCl} [g^{-1} cm^3]	0.6
ρ_P [mg ml^{-1}]	820
λ [Å s^{-1}]	$\cong$O(10)
pH	4.5

Table 1: Properties

5. REFERENCES

[1] F. Rosenberger, 'Inorganic and protein crystal growth: similarities and differences', J. Cryst. Growth 76, 618-636, (1986).

[2] A. McPherson, 'Current approaches to macromolecular crystallization', Eur. J. Biochem, 189, 1-23, (1990).

[3] F. Otàlora, J.M. Garcìa-Ruiz, 'Crystal growth studies in microgravity with the APCF: Computer simulation and transport dynamics', J. Cryst. Growth, 182, 141-154, (1997).

[4] S.R. Coriell, A.A. Chernov, B.T. Murray, G.B. McFadden, "Step bunching: generalized kinetics", Journal of Crystal Growth 183, 669-682, (1998).

[5] M.L. Pusey, R.S. Snyder, R. Naumann, 'Protein crystal growth: growth kinetics for tetragonal lysozyme crystals', Journal of Biological Chemistry, 261 (14), 6524-6529, (1986).

[6] A. Monaco, F. Rosenberger, 'Growth and etching kinetics of tetragonal lysozyme', J. Cryst. Growth, 129, 465-484, (1993).

[7] F. Otàlora, M.L. Novella, J.A. Gavira, B.R. Thomas, J.M. Garcìa-Ruiz, 'Experimental evidence for the stability of the depletion zone around a growing protein crystal under microgravity', Acta Crys., D57, 412-417, (2001).

[8] P. G. Vekilov, A. A. Chernov, "The Physics of Protein Crystallization, Solid State Physics", Vol 57, Ed H.Ehrenreich and F.Spaepen (Academic Press, Amsterdam, 2002) 1-147

[9] O. Galkin, P. G. Vekilov, "Direct determination of the nucleation rates of protein crystals", J. Phys. Chem. B 103, 10965-10971, (1999).

[10] M. Lappa, R. Savino, "3D analysis of crystal/melt interface shape and Marangoni flow instability in solidifying liquid bridges", J. Comput. Physics 180, 751-774, (2002).

[11] V.R. Voller, C. Prakash, 'A fixed grid numerical modelling methodology for convection-diffusion mushy region phase-change problems', Int. J. Heat Mass Transfer, 30 (8), 1709-1719, (1987).

[12] W.D. Bennon, F.P. Incropera, 'A continuum model for momentum, heat and species transport in binary solid-liquid phase change systems-I. Model formulation', Int.J.Heat Mass Transfer, 30 (10), 2161-2170, (1987).

[13] D. S. Noh, Y. Koh, I.S. Kang, 'Numerical solutions for shape evolution of a particle growing in axisymmetric flows of supersaturated solution', J. Cryst. Growth, 183, 427-440, (1998).

[14] H. Lin, F. Rosenberger, J.I.D. Alexander, A. Nadarajah, 'Convective-diffusive transport in protein crystal growth', J. Cryst. Growth, 151, 153-162, (1995).

[15] M. Lappa, "Growth and Mutual Interference of Protein Seeds under reduced gravity conditions", Phys. Fluids 15 (4), 1046-1057, (2003). This article has been also selected by the American Physical Society for the 15 March 2003 issue of the Virtual Journal of Biological Physics Research (Volume 5, Issue 6).

[16] M. Lappa, C.Piccolo, L. Carotenuto, "Numerical and experimental analysis of periodic patterns and sedimentation of lysozyme", J. Cryst. Growth, 254/3-4, 469-486, (2003).

[17] H.K. Henisch, J.M. Garcìa-Ruiz, "Crystal growth in gels and Liesegang ring formation: Crystallization criteria and successive precipitation", J. Cryst. Growth, 75, 203-211, (1986).

[18] H.K. Henisch, "Periodic Precipitation: a microcomputer analysis of transport and reaction processes in diffusion media with software development", Pergamon Press (1991).

[19] M. Lappa, D. Castagnolo, "Complex dynamics of rhythmic patterns and sedimentation of organic crystals: a new numerical approach", Num. Heat Transfer Part B - Fundamentals 43 (4), 373-401, (2003).

[20] M. Lappa, D. Castagnolo, L. Carotenuto, "Sensitivity of the non-linear dynamics of lysozyme 'Liesegang Rings' to small asymmetries", Physica *A,* 314/1-4, 623-636, (2002).

[21] M. Lappa, L. Carotenuto, "Effect of convective disturbances induced by g-jitter on the periodic precipitation of lysozyme ", Microgravity Science & Technology XIV/2, 41-56, (2003).

[22] C. Piccolo, M. Lappa, A. Tortora, L. Carotenuto, "Non-linear behaviour of lysozyme crystallization", Physica A 314/1-4, 636 - 645, (2002)

[23] L. Carotenuto, C. Piccolo, D. Castagnolo, M. Lappa, J.M. Garcìa-Ruiz, "Experimental observations and numerical modeling of diffusion-driven crystallization processes", Acta Cryst. D58, 1628-1632, (2002).

[24] D. Gueyffier, J. Li, A. Nadim, S. Scardovelli, S. Zaleski, 'Volume of Fluid interface tracking with smoothed surface stress methods for three-dimensional flows', J. Comput. Phys., 152, 423-456, (1999).